BIOORGANIC CHEMISTRY **24,** 110–126 (1996)
ARTICLE NO. 0011

Characterization of Products from the Reactions of Dopamine Quinone with *N*-Acetylcysteine

RONGDA XU,* XIN HUANG,* KARL J. KRAMER,† AND M. DALE HAWLEY*

**Department of Chemistry, Kansas State University, Manhattan, Kansas 66506; and †U.S. Grain Marketing Research Laboratory, Agricultural Research Services, United States Department of Agriculture,[1] Manhattan, Kansas 66502*

Received August 3, 1995

The reactions between electrochemically prepared dopamine (DA) quinone and *N*-acetylcysteine (NACySH), a protein model nucleophile, have been investigated at pH 7 and pH 2. Major products were purified by semipreparative reversed-phase liquid chromatography and identified by mass spectrometry and nuclear magnetic resonance spectroscopy to be nucleophilic addition products of the quinone with NACySH. The principal product is the monoaddition adduct of the quinone at C(5) of the ring, 5-*S*-(*N*-acetylcysteinyl)dopamine. The diaddition adduct of the quinone at C(2) and C(5) of the ring, 2,5-*S*,*S*′-di-(*N*-acetylcysteinyl)dopamine, and the monoaddition product at C(2) of the ring, 2-*S*-(*N*-acetylcysteinyl)dopamine, are produced to lesser extents. The relative molar ratio of 2-*S*-(*N*-acetylcysteinyl)dopamine, 5-*S*-(*N*-acetylcysteinyl)dopamine, and 2,5-*S*,*S*′-di-(*N*-acetylcysteinyl)dopamine produced at pH 7 is approximately 8:59:33, whereas at pH 2 the ratio is 10:89:1. The uv/vis spectroscopic analysis shows that the two monoaddition products have maxima at 258 and 294 nm, whereas the diaddition product has a maximum at 276 nm and a shoulder at 302 nm. Cyclic voltammetry and chronoamperometry demonstrate that these adducts are oxidized more readily than DA, which causes the anodic current for the oxidation of DA in the presence of NACySH to be kinetically controlled by the rates of the addition reactions. A reaction scheme is proposed for the formation of these products.

INTRODUCTION

Metabolism of dopamine (DA),[2] which is a neurotransmitter in the central nervous system of humans and other vertebrate animals, normally involves the formation of 3-methoxytyramine via *O*-methylation, 3,4-dihydroxyphenylacetic acid and 4-hydroxy-3-methoxyphenylacetic (homovanillic) acid via oxidative deamination, and norepinephrine via β-hydroxylation (*1*). In insects, DA is a neurotransmitter and is *N*-acylated to *N*-acetyldopamine and *N*-β-alanyldopamine, the main precur-

[1] The Agricultural Research Service, USDA is an equal opportunity/affirmative action employer and all agency services are available without discrimination.

[2] Abbreviations used: DA, dopamine; NACySH, *N*-acetylcysteine; LC, liquid chromatography; FAB–MS, fast atom bombardment mass spectrometry; NMR, nuclear magnetic resonance spectroscopy; CV, cyclic voltammetry; CA, chronoamperometry; EC, electrochemical detector; DEPT, distortionless enhancement by polarization transfer; 5-NACyS-DA, 5-*S*-(*N*-acetylcysteinyl)dopamine; 2-NACyS-DA, 2-*S*-(*N*-acetylcysteinyl)dopamine; 2,5-di-NACyS-DA, 2,5-*S*,*S*′-di-(*N*-acetylcysteinyl)dopamine.

0045-2068/96 $18.00

sors for quinonoid metabolites involved in sclerotization reactions that lead to adduct and cross-link formation with proteins (*2*). In addition, oxidation of DA to DA quinone is often observed (*3*). In insects at physiological pH, oxidation of DA can involve an intramolecular cyclization reaction that ultimately leads to the formation of a black, insoluble melanin polymer for pigmentation of the cuticle (*2*). Dopamine oxidation and melanin formation might also be associated with Parkinson's disease, where DA-containing cells in the nervous system are susceptible to degeneration (*4*, *5*). DA quinone can also react with nucleophiles such as glutathione, cysteine (*6*, *7*), and sulfhydryl groups in proteins (*8*, *9*). Some of these reactions occur physiologically; for example, the nucleophilic addition product, 5-*S*-cysteinyldopamine, has been detected in striatal tissue from various species (*10*).

The reactions of DA quinone with L-cysteine at physiological pH have been studied previously by continuously electrolyzing a mixture of DA and excess L-cysteine (*11*). Since the initial cysteinyl adducts are oxidized to their corresponding quinones at the applied potential, and since the amine moiety of the cysteinyl adduct also functions as a nucleophile, numerous products were formed, many of which were not identified.

The goal of our work was to clarify the initial steps of the oxidation reaction pathway of DA when a model protein nucleophile is present in excess. To determine the initial site(s) of nucleophilic attack on DA quinone, DA was first oxidized in the absence of a nucleophile to produce DA quinone. The electrolysis was terminated before mixing DA quinone with a nucleophile. This procedure minimizes the generation of additional oxidation products that would be formed if excess chemical oxidant were used to oxidize DA or if exhaustive electrolysis of DA were carried out in the presence of a nucleophile. Since the amino group in cysteine and cysteinyl adducts can act as a nucleophile (*11*), the amino group was acetylated in order to render it unreactive.

Products from the reactions of DA quinone with NACySH were analyzed using reversed-phase liquid chromatography (LC). The major products were purified using semipreparative LC and characterized by fast atom bombardment mass spectrometry (FAB–MS), nuclear magnetic resonance spectroscopy (NMR), uv/vis spectroscopy, and cyclic voltammetry (CV). CV was used to characterize the electrochemical behavior of this system. Rate constants for the addition reactions were estimated using chronoamperometry (CA).

MATERIALS AND METHODS

Chemicals

The following chemicals were obtained from commercial sources and used as received: DA and NACySH (Sigma Chemical Co., St. Louis, MO);[3] formic acid, ammonium formate and disodium ethylenediaminetetraacetate (EDTA) (Fisher Scientific Co., Pittsburgh, PA); methanol (uv cutoff: 204 nm) (Baxter Healthcare

[3] Mention of a proprietary product does not constitute a recommendation by the USDA.

Corporation, Burdick & Jackson Division, Muskegon, MI); KCl (Mallinckrodt Specialty Chemicals, Chesterfield, MO); and HCl (J. T. Baker Chemical Co., Phillipsburg, NJ).

Electrochemical Preparation of DA Quinone

DA was oxidized in 0.01 M HCl and 0.09 M KCl (pH 2.0) in a custom-made coulometric cell. A platinum gauze working electrode and a Ag/AgCl (saturated KCl) reference electrode were placed in the sample compartment. A platinum auxiliary electrode was separated from this compartment by means of a 0.45-μm nylon 66 membrane so that electrolysis could be conducted efficiently and without mixing of the anode and cathode reaction products. A custom-built three-electrode potentiostat was used to apply a constant potential and to give instantaneous analog current and digital coulomb readouts (*12*). The potential for coulometric oxidation of DA was controlled at 700 mV vs Ag/AgCl (saturated KCl). Electrolysis was terminated when the current-time curve reached a plateau value, indicating that DA oxidation was complete. Electrolysis for 3 min was sufficient for complete oxidation (>99%) of 0.5 ml of 1 mM DA. DA quinone was found to be relatively stable at pH 2.0 in a separate uv spectrophotometric experiment with the decrease in absorbance at 390 nm being less than 0.75% after 3 min (Huang *et al.,* unpublished data).

Analytical LC and Electrochemical Studies of the Reactions of DA Quinone with NACySH

The compositions of reaction mixtures that resulted from mixing 0.4 ml 1 mM DA quinone with 0.2 ml 10 mM NACySH at either pH 7.4 or pH 2.0 were analyzed by LC. The LC system consisted of a Beckman (Berkeley, CA) Model 332 gradient liquid chromatography system equipped with two Model 110A pumps and a Model 420 controller, a Hewlett–Packard (Palo Alto, CA) HP 8452A diode array spectrophotometer equipped with a 1-cm quartz flow cell (Pyrocell Manufacturing Co., Inc., Westwood, NJ), and a Bioanalytical Systems (West Lafayette, IN) LC-4B dual amperometric detector connected to a Hewlett–Packard HPLC ChemStation via a Hewlett–Packard 35900 multichannel interface. The uv/vis spectra of the LC effluent were recorded every 10 s for the duration of the experiment within the 220- to 800-nm wavelength range. The dual amperometric detector that was used for electrochemical detection of the LC effluent consisted of two glassy carbon working electrodes, a Ag/AgCl (3 M KCl) reference electrode, and a stainless steel auxiliary electrode. Electrode potentials were 800 and −100 mV. The former potential is sufficient to oxidize DA and all *N*-acetylcysteinyl adducts of DA, whereas the latter potential is sufficient to reduce DA quinone and all adduct quinones. The two working electrodes were arranged in a parallel configuration so that both electrochemically oxidizable species and reducible species in the LC effluent could be detected simultaneously. Two chromatograms were recorded from the electrochemical (EC) detector and are referred to as LC–EC (oxidation) and LC–EC (reduction) chromatograms. Separation was achieved on a Microsorb-MV C18 column (5 μm, 4.6 × 250 mm) (Rainin Instrument Co., Inc., Woburn, MA) with a binary mobile phase system in which solvents A and B were used. Solvent

A was 150 mM formic acid, 30 mM ammonium formate, and 0.1 mM EDTA (pH 3.0), and solvent B was 50% methanol, 180 mM formic acid, 8 mM ammonium formate, and 0.1 mM EDTA (pH 3.0). The mobile phase gradient was 0 min, 95% solvent A and 5% solvent B; 0–30 min, linear gradient from 5% solvent B to 30% solvent B; 30–40 min, linear gradient from 30% solvent B to 100% solvent B. The flow rate was at 1 ml/min; a 180-μl sample injector loop was used.

A Bioanalytical Systems BAS-100W electrochemical system was used to perform CV and CA. A BAS glassy carbon electrode with an area of 7.1 mm^2 was used as the working electrode. The reference and auxiliary electrodes were a Ag/AgCl (saturated KCl) electrode and a Pt wire electrode, respectively. A small electrochemical cell with a capacity of 1 ml was used. CV of 0.3 mM DA in the presence of 0, 0.3, or 1.5 mM NACySH in 0.1 M phosphate buffer (pH 7.0) and 0.3 mM DA in the presence of 0 or 3.0 mM NACySH in 0.01 M HCl and 0.09 M KCl (pH 2.0) was carried out. The scan rate was 200 mV/s. CA data were acquired for 0.3 mM DA in the absence and presence of 3.0 mM NACySH. The potential was stepped from −0.2 to 0.6 V when in 0.1 M phosphate buffer at pH 7.0 and from 0 to 0.8 V when in 0.01 M HCl and 0.09 M KCl at pH 2.0. These oxidation potentials were sufficiently positive to oxidize DA and all *N*-acetylcysteinyl adducts under these experimental conditions.

Synthesis and Purification of Products from Reaction of DA Quinone with NACySH

A DA quinone solution, prepared by the electrolysis of 10 ml 15 mM DA in 0.01 M HCl and 0.09 M KCl, was added dropwise to 5 ml 150 mM NACySH in 0.5 M phosphate buffer (pH 7.4). The final reaction mixture was colorless and its pH remained at 7.4. The reaction mixture was lyophilized to reduce the volume, and the concentrated solution was filtered and subjected to a semipreparative LC separation. The LC system described above was used, but with the electrochemical detector disconnected. Separation was achieved on a Phenomenex (Torrance, CA) C18 semipreparative column (10 μm, 250 × 10 mm). The mobile phase gradient employed was 0 min, 95% solvent A and 5% solvent B; 0–40 min, linear gradient from 5% solvent B to 40% solvent B. The flow rate was 4 ml/min; a 5-ml sample loop was used. Each product effluent was collected and subjected to a desalting step using the semipreparative LC column. After a product solution was injected onto the column, the salt components were eluted first using distilled water as the mobile phase; the product was then eluted using 25% methanol. The effluent containing the product was subsequently lyophilized to dryness.

Characterization of Products

FAB–MS was performed on a Hewlett–Packard HP 5989A MS Engine. Proton NMR and distortionless enhancement by polarization transfer (DEPT) NMR were performed with a Varian (Palo Alto, CA) UNITY*plus* 400 MHz spectrometer. Products were dissolved in 0.8 ml D_2O. The uv/vis spectroscopic measurements of the reaction products in 0.01 M HCl were performed using the HP 8452A diode-array spectrophotometer with a 1.0 × 0.4-cm quartz cuvette. Cyclic voltammograms

of reaction products in 0.1 M phosphate buffer (pH 7.0) were obtained using the BAS-100W electrochemical system. The scan rate was 200 mV/s.

RESULTS

LC Analysis of Reaction Products of DA Quinone with NACySH

The products obtained from mixing 0.4 ml 1 mM DA quinone with 0.2 ml 10 mM NACySH at either pH 7.4 or pH 2.0 were separated by analytical LC. No discernible peaks were observed in the LC–EC (reduction) chromatograms (data not shown). Four major peaks and several minor peaks were obtained in the LC–EC (oxidation) chromatogram for the reaction conducted at pH 7.4 (Fig. 1A). The peak at 7.26 min is due to DA (**1,** see Scheme 1), while the peaks at 11.23, 21.24, and 25.62 min are due to three major reaction products, identified here as compounds **3, 4,** and **7,** respectively. The same products are observed at pH 2.0, but two of the products, **1** and **7,** are formed in much lower yields than at pH 7.4 (Fig. 1B). The minor peak at 9.1 min is due to NACySH, whereas the minor peak at 8.2 min is due to an impurity in the starting material. The other minor peaks are unidentified.

NMR and MS Identification of Reaction Products

Products **3, 4,** and **7** were first characterized by FAB–MS. The results showed that **3** and **4** both have MH^+ at m/z=315 and that **7** has MH^+ at m/z=476 (spectra not shown). These results strongly suggest that **3** and **4** are both monoaddition adducts (theoretical m/z: 315) of NACySH with DA quinone, whereas **7** is a diaddition adduct of two NACySH molecules with DA quinone (theoretical m/z: 476).

The structures of these adducts were elucidated by NMR spectroscopy (Table 1). The ^{1}H NMR spectrum of **4** shows that the molecule contains two aromatic protons that give *meta*-coupling (J = 2.0 Hz) (Fig. 2A). Because this result indicates that the *N*-acetylcysteinyl moiety is bound to C(5) of the aromatic ring of DA, **4** is identified as 5-*S*-(*N*-acetylcysteinyl)dopamine (5-NACyS-DA). The ^{1}H NMR spectrum of **3** shows that the molecule contains two aromatic protons that display *ortho*-coupling (J = 8.2 Hz), indicating that the *N*-acetylcysteinyl moiety is bound to C(2) of the aromatic ring of DA (Fig. 2B). Therefore, **3** is identified as 2-*S*-(*N*-acetylcysteinyl)dopamine (2-NACyS-DA).

The ^{1}H NMR spectrum of the diaddition adduct **7** shows only a singlet in the aromatic region (Fig. 2C), which suggests that both of the *N*-acetylcysteinyl moieties are attached to the aromatic ring of DA. Since the signals of the DA side chain protons overlap with the signals of the protons in the *N*-acetylcysteinyl moiety in this ^{1}H NMR spectrum, a DEPT NMR experiment was conducted to confirm that the *N*-acetylcysteinyl moieties are not attached to the DA side chain carbons (Fig. 3). The DEPT NMR spectrum exhibits four 180° out-of-phase signals, demonstrating that four $-CH_2-$ groups are present in the molecule, two of which are in the two *N*-acetylcysteinyl moieties and two of which are in the DA side chain. This confirms that both *N*-acetylcysteinyl moieties are bound to the aromatic ring of DA. Based on the fact that there is little or no 6-monoaddition product present in the reaction

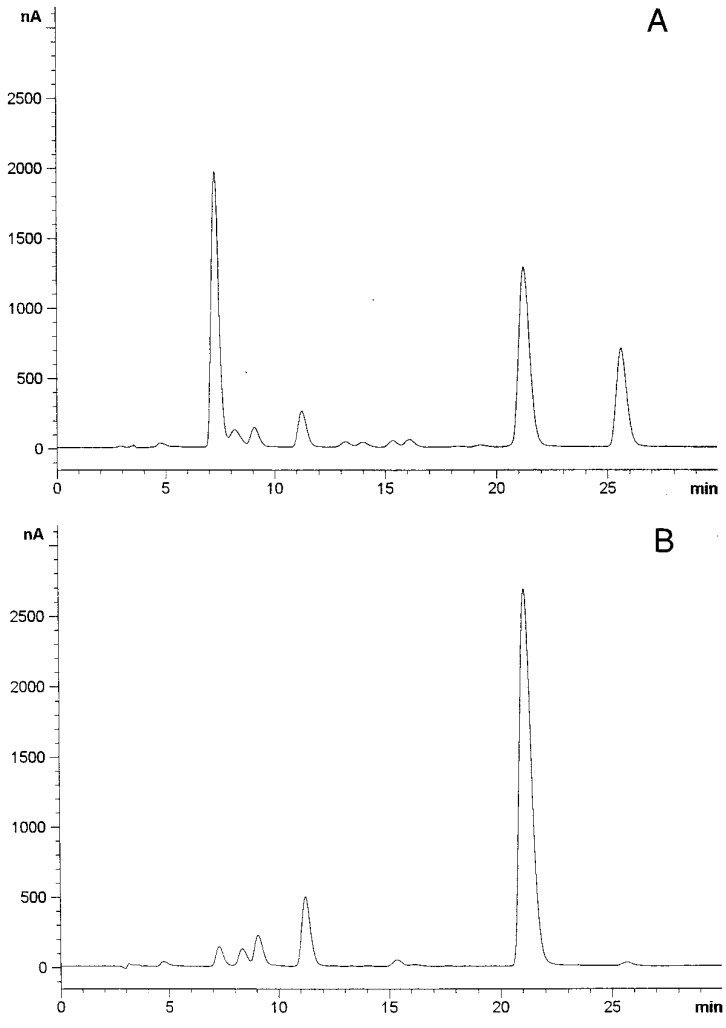

FIG. 1. LC–EC (oxidation) chromatograms of the reaction products of DA quinone and NACySH at (A) pH 7.4 and (B) pH 2.0.

mixture, C(6) of the DA quinone ring is presumed to be the site that is least reactive with NACySH. Accordingly, because assignments where two *N*-acetylcysteinyl moieties are bound to the 2,6-carbons or 5,6-carbons of the DA aromatic ring are excluded, the two *N*-acetylcysteinyl moieties must be bound to C(2) and C(5) of the DA aromatic ring in adduct **7.** This species is identified as 2,5-*S*,*S*′-di-(*N*-acetylcysteinyl)dopamine (2,5-di-NACyS-DA).

The uv/vis and Electrochemical Characterization of the Reaction Products

The adducts were also characterized using uv/vis spectrometry and CV. The uv/vis spectra show that, whereas both monoaddition adducts (**3** and **4**) have the

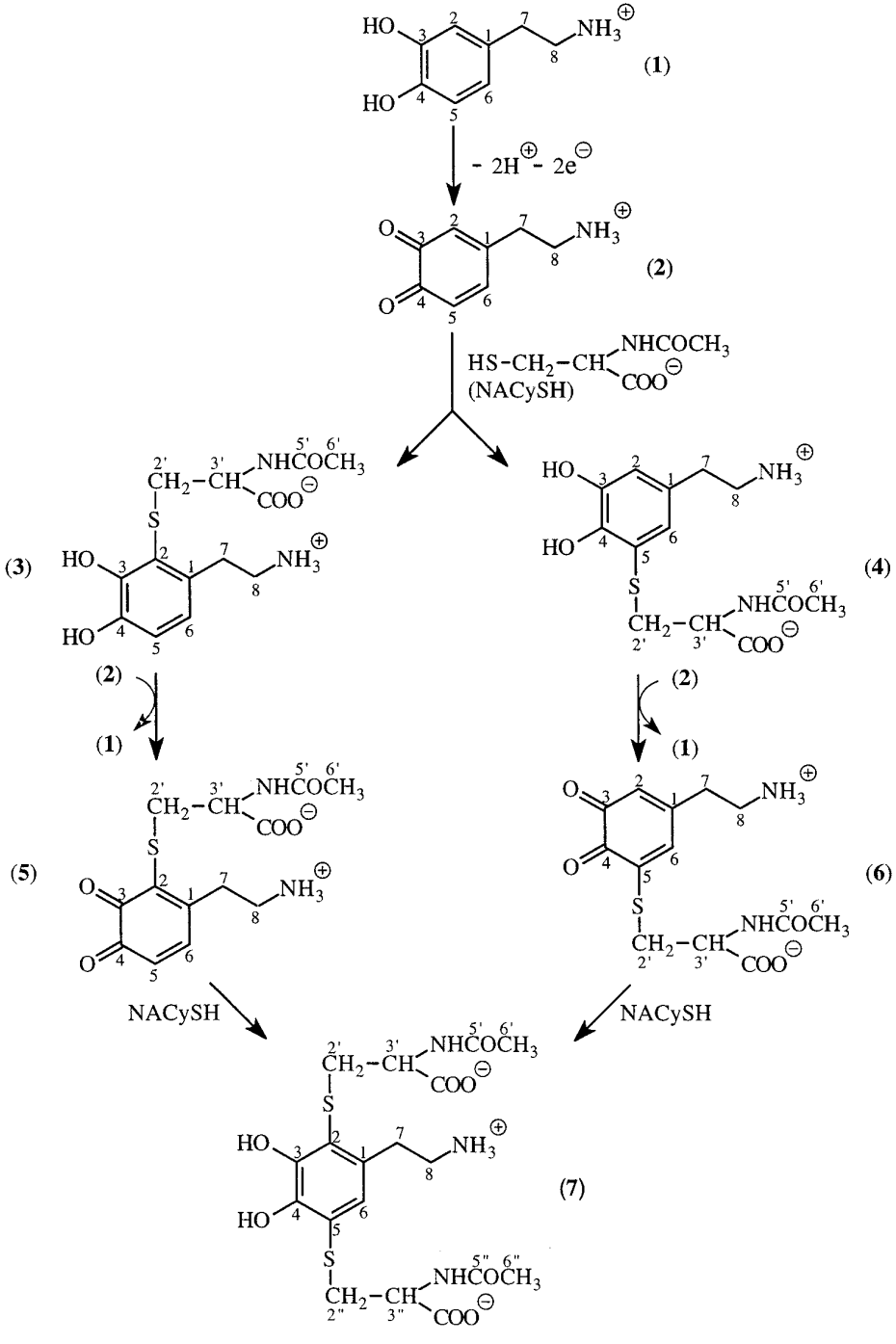

SCHEME 1. Proposed mechanism for formation of adducts from reactions of DA quinone with NACySH.

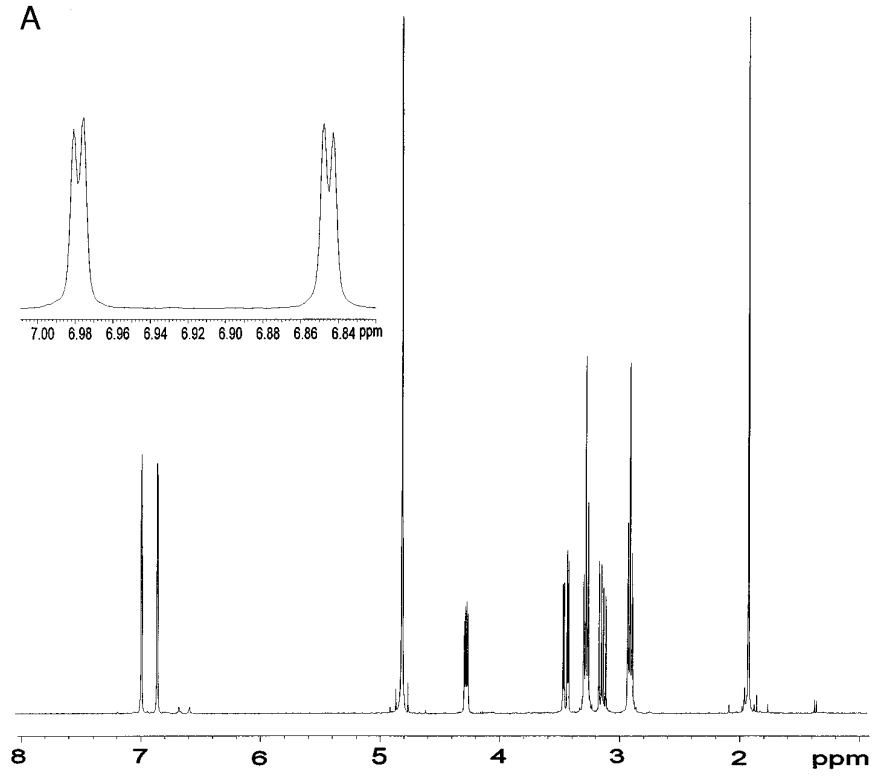

FIG. 2. ^{1}H NMR spectra of addition products from reaction of DA quinone with NACySH: (A) monoaddition product 5-NACyS-DA (**4**), (B) monoaddition product 2-NACyS-DA (**3**), and (C) diaddition product 2,5-di-NACyS-DA (**7**).

same λ_{max} values, 258 and 294 nm, they have different molar absorption coefficients at each λ_{max} (Table 2). In contrast, the diaddition adduct (**7**) has only one λ_{max} at 276 nm and a shoulder at 302 nm. CV data show that all three adducts have slightly less positive redox potentials than DA at pH 7.0, indicating that they would be readily oxidized by any unreacted DA quinone in the reaction mixture (Table 2). Other characteristic data of these adducts are also presented in Table 2.

To estimate the relative molar ratios of adducts **3, 4,** and **7** formed at pH 7.4 and pH 2.0, LC–UV chromatograms (absorbance at λ_{max} versus time) of the reaction mixtures were obtained (not shown). Based on the peak areas and respective molar absorption coefficients, the relative molar ratios of adducts **3, 4,** and **7** are estimated to be 8:59:33 at pH 7.4 and 10:89:1 at pH 2.0.

Electrochemical Studies of DA in the Presence of NACySH

The cyclic voltammogram of DA at pH 7.0 in the absence of NACySH consists of a single anodic peak near 0.26 V for the two-electron oxidation of DA to its corresponding quinone and a single cathodic peak near 0.13 V for the reduction

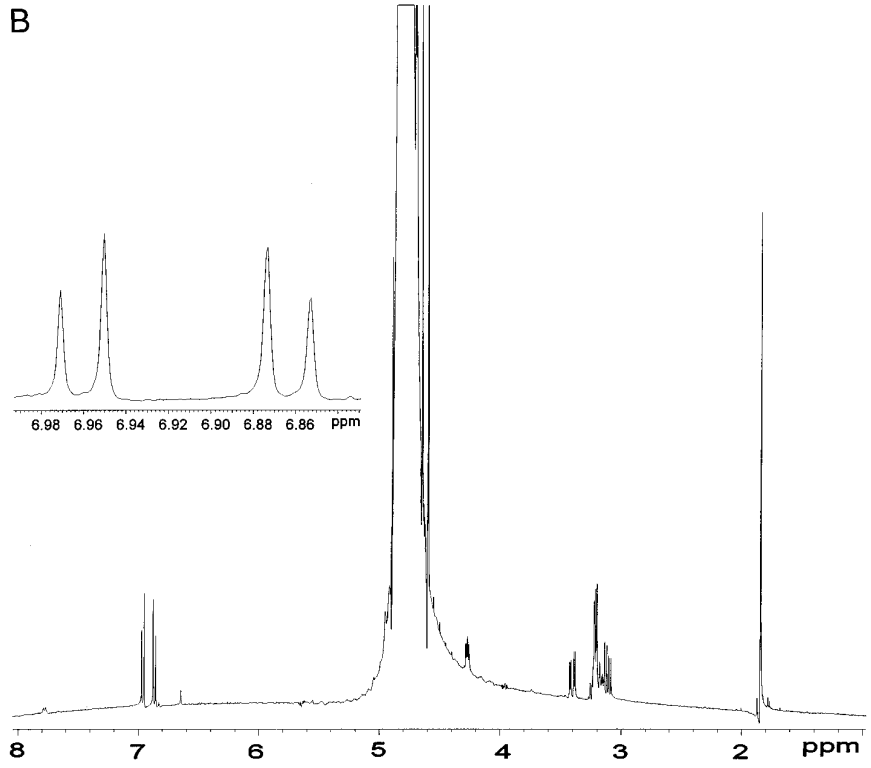

FIG. 2—*Continued*

of the quinone to starting material (Fig. 4A). The absence of any other discernible redox process indicates that DA quinone is relatively stable under these conditions (pH 7.0, scan rate: 200 mV/s). In the presence of an equimolar amount of NACySH, the anodic peak for the oxidation of DA nearly doubles in height (Fig. 4B). Concomitantly, the magnitude of the cathodic peak for the redox of DA quinone is reduced substantially. The cathodic peak for the reduction of DA quinone is eliminated completely when the ratio of NACySH to DA is five (Fig. 4C).

The absence of a cathodic peak in the cyclic voltammogram of DA in the presence of a fivefold excess of NACySH is probably due to either the quinone being consumed by the nucleophile or the nucleophile transferring electrons to the quinone. To determine which of these possibilities is occurring, the nucleophile was added to a solution of electrochemically prepared diadduct quinone. If an electron-transfer process were to occur between the quinone and the nucleophile, the diadduct quinone would be reduced and the nucleophile would be oxidized. On the other hand, if a nucleophilic reaction were to occur between the quinone and the nucleophile, a new species would be formed, which should be detected by LC analysis.

After the diadduct, 2,5-di-NACyS-DA, was partially oxidized electrochemically, the resulting quinone was then mixed with NACySH. The chromatogram of the NACySH/quinone mixture had one additional major anodic peak at 21.2 min in

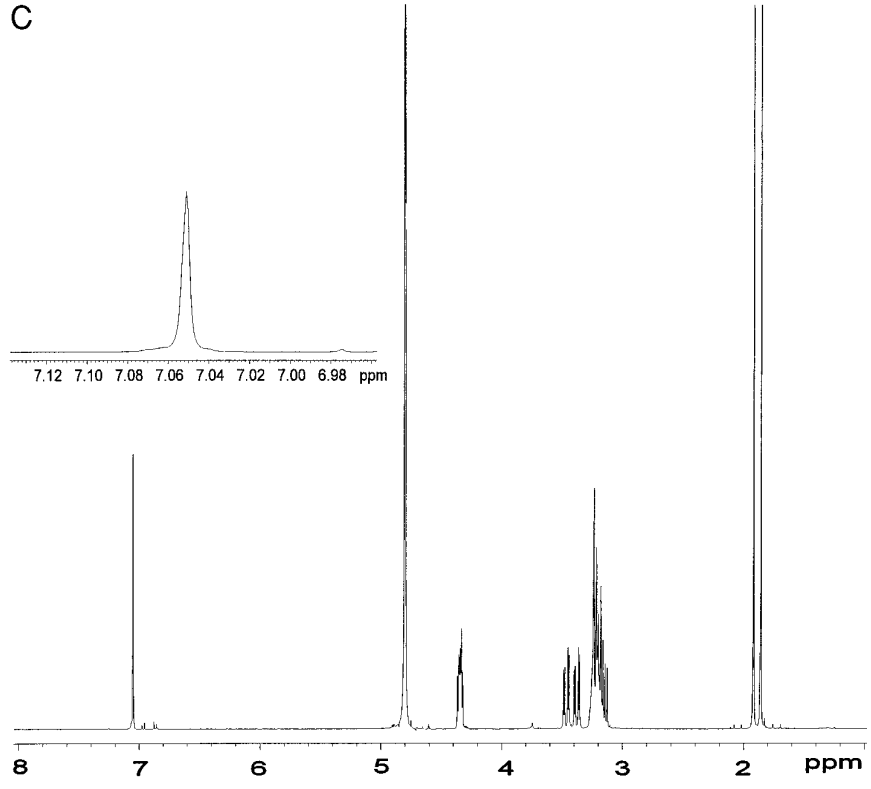

FIG. 2—*Continued*

addition to the diadduct peak at 13.0 min (data not shown). The effluent that gives rise to this additional peak exhibits a λ_{max} at 309 nm and a shoulder at 323 nm in its uv/vis spectrum (data not shown), which is consistent with the formation of the triadduct, 2,5,6-tri-NACyS-DA. Addition of the NACyS- group to the aromatic ring would be expected to cause a red shift in the λ_{max}: DA, 202 and 280 nm; 2- or 5-NACyS-DA, 258 and 294 nm; and 2,5-di-NACyS-DA, 276 and 302 nm. These

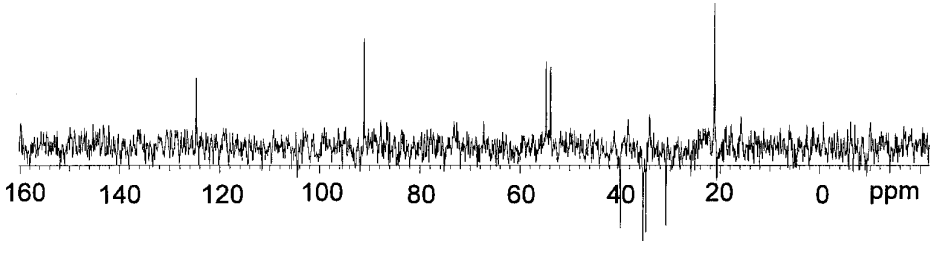

FIG. 3. DEPT NMR spectrum of diaddition product 2,5-di-NACyS-DA (**7**) from reaction of DA quinone with NACySH.

TABLE 1
^{1}H NMR Data and Structural Assignments of NACySH Adducts of DA[a]

2-NACyS-DA (**3**)			5-NACyS-DA (**4**)			2,5-di-NACyS-DA (**7**)		
δ (ppm)	Coupling (Hz)	Assignment	δ (ppm)	Coupling (Hz)	Assignment	δ (ppm)	Coupling (Hz)	Assignment
6.96	d(8.24)	H5	6.98	d(2.13)	H2	7.05	s	H6
6.86	d(8.24)	H6	6.84	d(1.84)	H6	4.34	m	H3′, 3″
4.27	dd(7.17, 3.97)	H3′	4.26	dd(8.24, 3.97)	H3′	3.47	dd(14.34, 4.27)	H2′a (or 2″a)
3.40	dd(13.74, 3.97)	H2′a	3.40	dd(14.34, 3.97)	H2′a	3.38	dd(13.88, 4.28)	H2″a (or 2′a)
3.21	m	H7, 8	3.27	t(7.02)	H8	3.22	m	H7, 8, 2′b, 2″b
3.11	dd(14.04, 7.32)	H2′b	3.14	dd(14.35, 8.24)	H2′b	1.92	s	H6″
1.84	s	H6′	2.90	t(7.02)	H7	1.86	s	H6′
			1.91	s	H6′			

[a] Data were measured in D_2O at 27°C, using HOD (δ 4.8 ppm) as a reference signal. See Scheme 1 for structures of the adducts.

data suggest that NACySH reacts with 2,5-di-NACyS-DA quinone primarily by nucleophilic addition to form a triadduct, rather than by reduction to regenerate the diadduct starting material. To demonstrate that there is no additional anodic peak at 21.2 min when the quinone is reduced, a separate experiment was conducted in which an electron acceptor, ascorbic acid, was added to a solution of the diadduct quinone. As expected, the LC chromatograms exhibited only one major anodic peak at 13.0 min, which is due to the reduced diadduct (data not shown).

These results demonstrate that (1) DA quinone reacts rapidly with NACySH to give a species that is oxidizable at the applied potential and (2) all electrogenerated quinones are consumed under these conditions by follow-up chemical reactions.

TABLE 2
Characteristic Data of DA and Its NACySH Adducts

Compound[a]	M_r[b]	RT (min)[c]	Relative yield[d]	UV: λ_{max} (log ε)[e]	CV: E_{pa}, E_{pc} (mV)[f]
DA (**1**)	153	6.21	n/a	202 (3.43), 280 (3.41)	255, 125
2-NACyS-DA (**3**)	314	8.87	8%	258 (3.43), 294 (3.41)	228, 134
5-NACyS-DA (**4**)	314	13.74	59%	258 (3.49), 294 (3.36)	179, 133
2,5-di-NACyS-DA (**7**)	475	15.14	33%	276 (3.95), 302 (sh, 3.46)	226, 105

[a] See Scheme 1 for structures of the adducts.

[b] The molecular weights were determined using FAB–MS.

[c] Retention times were obtained from the LC–EC chromatogram of the reaction mixture at pH 7.4 (Fig. 1A).

[d] The relative yields of the three major products were estimated on the basis of their peak areas in the LC–DAD chromatogram (not shown) of the reaction mixture at pH 7.4 and their molar absorption coefficients[e].

[e] The uv/vis molar absorption coefficients of products were obtained in 0.01 M HCl (Fig. 4).

[f] Cyclic voltammetric data were obtained on a 7.1-mm^2 glassy carbon electrode at a scan rate of 200 mV/s in 0.1 M phosphate buffer at pH 7.0 (Fig. 5).

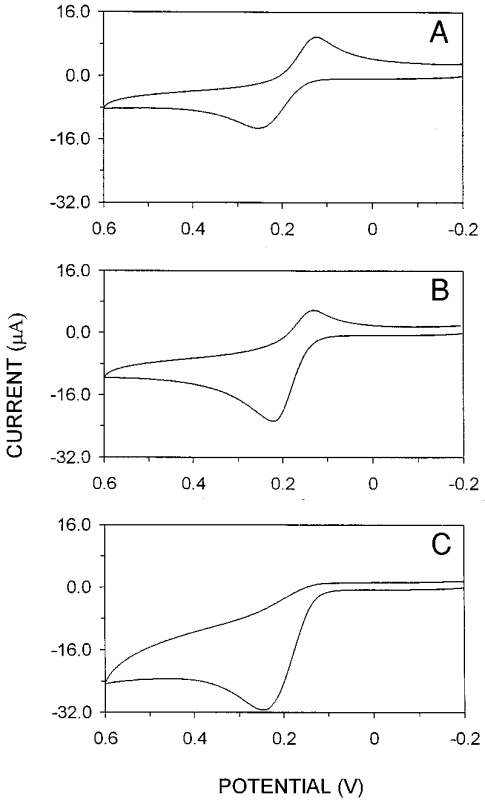

FIG. 4. Cyclic voltammograms of 0.3 mM DA in the presence of (A) 0 mM, (B) 0.3 mM, and (C) 1.5 mM NACySH in 0.1 M phosphate buffer (pH 7.0). The scan rate was 200 mV/s.

Although the absence of the cathodic current during the reversed scan is not fully understood, it might be due to the fact that multiple adducts are formed and that all of the quinones are consumed either by adduct formation or by acting as oxidants of the adducts.

Attempts to determine the rate constant of the initial reaction of DA quinone with NACySH at pH 7.0 by CA were unsuccessful. Although the apparent number of electrons transferred, n_{app}, for the oxidation of DA in the presence of NACySH was kinetically controlled, n_{app} exceeded 4.0 throughout the accessible time range of 100 ms $\leq t \leq$ 5 s when [NACySH]/[DA] = 10 (Fig. 5). This result permits lower limits of 100 s^{-1} and 3.3 $\times$ 10^4 M^{-1} s^{-1} to be set for the pseudo-first-order and second-order rate constants, respectively, for the initial reactions of NACySH with DA quinone (*13*), which are consistent with the estimation of 315 s^{-1} and 6.3 $\times$ 10^5 M^{-1} s^{-1} that Tse and co-workers have reported for the addition of cysteine to dopamine at pH 7.4 (*7*).

Even though the experiment is subject to several sources of error, the variation of n_{app} from a value near 4.0 when t = 100 ms to 5.8 when t = 5 s suggests that

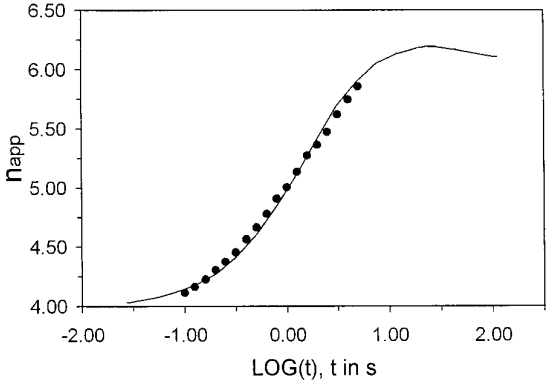

FIG. 5. CA data and working curve for the addition of NACySH to NACyS-DA quinone in 0.1 M phosphate buffer (pH 7.0). Concentrations of DA and NACySH were 0.3 and 3.0 mM, respectively. Potential step was from −0.2 to 0.6 V vs. Ag/AgCl (saturated KCl). Working curve for ECE process (K = 10) for the reaction described by Eq. [5], —; experimental data, ●●●.

the rate constant for the addition of NACySH to NACyS-DA quinone might be amenable to estimation (Fig. 5). When n_{app} vs t was fit to the theoretical working curve for a homogeneous chemical reaction interposed between electron transfer reactions, a reasonable fit was obtained when $k = 0.76\ s^{-1}$ was used for the pseudo-first-order rate constant and $k' = k/[\text{NACySH}] = 2.5 \times 10^2\ M^{-1}\ s^{-1}$ for the second-order rate constant. The theoretical working curve was obtained by digital simulation of the sequence of reactions that is described by Eqs. [1] to [5].

$$\text{DA} \rightleftharpoons \text{DA quinone} + 2\text{H}^+ + 2\ \text{e}^- \quad [1]$$

$$\text{DA quinone} + \text{NACySH} \xrightarrow{\text{fast}} \text{NACyS-DA} \quad [2]$$

$$\text{NACyS-DA} + \text{DA quinone} \xrightarrow{\text{fast}} \text{NACyS-DA quinone} + \text{DA} \quad [3]$$

$$\text{NACyS-DA quinone} + \text{NACySH} \xrightarrow{k'} (\text{NACyS})_2\text{-DA} \quad [4]$$

$$\text{NACyS-DA quinone} + (\text{NAcyS})_2\text{–DA} \overset{K=10}{\rightleftharpoons} \text{NACyS-DA} + (\text{NACyS})_2\text{-DA quinone} \quad [5]$$

The model assumes that reactions [1] through [3] occur rapidly and that reaction [4] is rate controlling. Since each of the electrochemical oxidations in reactions [1] and [3] involves two electrons per molecule of DA and NACyS–DA, the minimum value of n_{app} at small values of kt, where k is the pseudo-first-order rate constant and t is time, should be 4.0. In contrast, when kt is large, a limiting value of 6.0 is predicted for this reaction sequence (*13*). The final two electrons per molecule of DA arise from the homogeneous redox reaction that is described by Eq. [5]. The value of the equilibrium constant for this reaction is based on the redox potentials

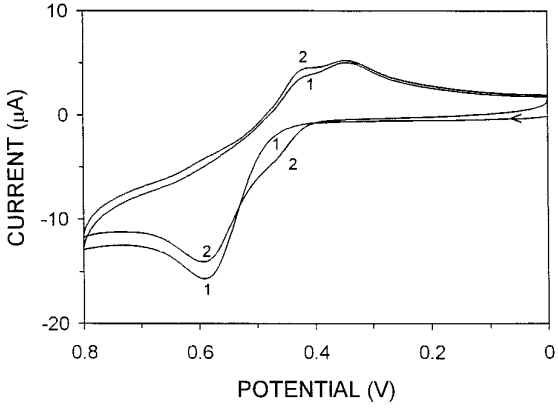

FIG. 6. Cyclic voltammogram of 0.3 mM DA in the presence of 3.0 mM NACySH in 0.01 M HCl and 0.09 M KCl (pH 2.0). The scan was initiated in the positive-going direction at a rate of 200 mV/s. The numbers 1 and 2 indicate the first and second cycles, respectively.

of DA and the monoadducts (see Table 2). Departure from semiinfinite linear diffusion at longer times limited our experimental time range to $t \leq 5$ s. Because NACySH is also oxidized slowly at the applied potential of 0.6 V, currents for the oxidation of DA in the presence of NACySH were corrected for this background process.

The rate of the initial reaction of NACySH with DA (Eq. [2]) is significantly slower at pH 2.0 than at pH 7.0. As shown in Fig. 6, the cyclic voltammogram consists of a single, kinetically controlled anodic peak for the oxidation of DA to DA quinone near 0.59 V on the first, positive-going sweep. Upon reversal of the potential scan at 0.80 V, the negative-going sweep consists of two cathodic peaks. The more positive of these peaks is due to the reduction of predominately 5-NACyS-DA quinone, whereas the more negative peak near 0.35 V is due to the reduction of unreacted DA quinone. On the second, positive-going sweep, a new anodic peak appears at 0.48 V, which is assigned to the two-electron oxidation of 5-NACyS-DA to 5-NACyS-DA quinone. As expected when the initial electrode product, DA quinone, is consumed by a follow-up chemical reaction to produce a new electroactive species, the relative magnitudes of the cyclic voltammetric peaks for the adduct redox couple, 5-NACyS-DA/5-NACyS-DA quinone, increase at the expense of the peaks for the DA/DA quinone redox couple with increasing number of cyclic voltammetric cycles. The observations that $E_{p,a}$ for 5-NACyS-DA occurs at a less positive potential than that for DA, whereas $E_{p,c}$ for 5-NACyS-DA quinone occurs at a more positive potential than that for DA quinone, are attributed to the greater electrochemical reversibility of the 5-NACyS-DA/5-NACyS-DA quinone redox couple than of the DA/DA quinone redox couple.

The rate constant for the reaction of DA quinone with NACySH at pH 2.0 was determined by CA. In the absence of NACySH, the oxidation of DA to DA quinone is a diffusion-controlled two-electron process. However, when [NACySH]/[DA] = 10, n_{app} is kinetically controlled, varying from its lower limit near 2.0 when $t = 100$

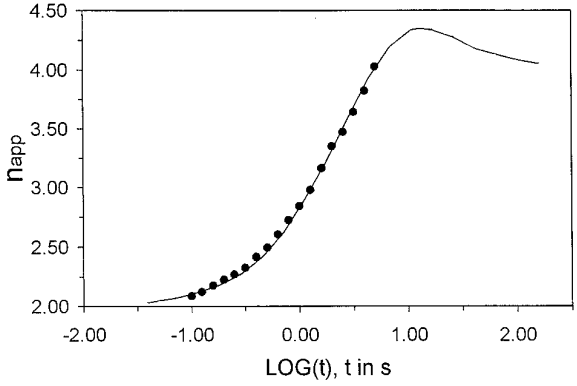

FIG. 7. CA data and working curve to estimate the rate constant for the addition of NACySH to DA quinone in 0.01 M HCl and 0.09 M KCl (pH 2.0). Concentrations of DA and NACySH were 0.3 and 3.0 mM, respectively. Potential step was from 0 to 0.8 V vs Ag/AgCl (saturated KCl). Working curve for ECE process ($K = 1$) for the reaction described by Eq. [6], —; experimental data, ●●●.

ms to 4.0 when $t = 5$ s. These data were then fit to the theoretical working curve for an ECE process in which a pseudo-first-order chemical reaction, the addition of NACySH to DA quinone (Eq. [2]), is interposed between the two-electron oxidations of DA (Eq. [1]) and 5-NACyS-DA (Eq. [3]) to DA quinone and 5-NACyS-DA quinone, respectively (*13*, Fig. 7). Values of 0.53 s^{-1} and 1.8×10^2 M^{-1} s^{-1} were calculated for the pseudo-first-order and second-order rate constants, respectively, for the reaction described by Eq. [2] at pH 2.0. The equilibrium constant that was used for the homogenous redox reaction was 1.0, which is based on the fact that $(E_{p,a} + E_{p,c})/2$ for both redox couples is 0.46 V at pH 2.0 (Eq. [6]).

$$\text{5-NACyS-DA quinone} + \text{DA} \overset{K=1}{\rightleftharpoons} \text{5-NACyS-DA} + \text{DA quinone} \qquad [6]$$

Again, since NACySH is also oxidized slowly at the applied potential of 0.8 V, the kinetically controlled current for oxidation of DA in the presence of excess NACySH in Fig. 7 was corrected for this background process.

DISCUSSION

Cyclic voltammetric studies have shown that the mono- and diaddition adducts of NACySH with DA quinone are oxidized more readily than DA at pH 7.0. Since our goal was to study the initial products that arise from the reaction of DA quinone with NACySH, electrolysis of DA was effected in the absence of added nucleophiles and was terminated when its oxidation was complete. DA quinone was determined to be stable under the conditions of its preparation, but was found to react rapidly when it was added to a solution of NACySH.

The most abundant product detected in our system is 5-NACyS-DA (**4**), the

monoaddition adduct of the quinone at C(5) of the ring of DA. The second major product produced at pH 7.4 is the diaddition adduct of the quinone bonded at C(2) and C(5) of the ring (2,5-di-NACyS-DA, **7**). In addition, we found that the monoaddition product linked at C(2) of the ring (2-NACyS-DA, **3**) is also produced at pH7.4, but at a lower yield than that of either 5-NACyS-DA or 2,5-di-NACyS-DA. The formation of 5-NACyS-DA is consistent with the detection of 5-*S*-cysteinyldopamine in a previous study where DA was electrolyzed in the presence of L-cysteine (*11*). However, the monoaddition adduct of the quinone bonded at C(2) of the ring of DA was not detected in that study, apparently because continuous electrolysis caused electrochemical oxidation of the initial products and formation of many other products. CV of DA in the presence of NACySH reveals a kinetically controlled anodic current that is the result of reactions of DA quinone with NACySH to yield adducts that are also electroactive at the applied potential.

Since electrolysis was terminated prior to the addition of NACySH, oxidation of the monoaddition adducts will be effected only by any DA quinone that remains unreacted. If the quinones of the monoaddition adducts were to react also with NACySH, the product distribution would be predicted to contain equimolar amounts of DA and the 2,5-di-NACyS-DA adduct. The experimental results are consistent with this expectation at both pH 2.0 and pH 7.4.

A pathway is proposed for the reaction of electrogenerated DA quinone with an excess of NACySH (Scheme 1). After DA quinone (**2**) is mixed with NACySH, nucleophilic attack of NACySH occurs on the ring of DA quinone principally at C(5) and to a lesser extent at C(2), to form 5-NACyS-DA (**4**) and 2-NACyS-DA (**3**), respectively. Portions of these two monoaddition adducts are subsequently oxidized by unreacted DA quinone to form the corresponding quinones of the monoaddition adducts (**5** and **6**) and to regenerate DA. 2-NACyS-DA quinone (**5**) and 5-NACyS-DA quinone (**6**) are then subject to nucleophilic attack by NACySH at the 5- and 2-positions of the ring, respectively, forming 2,5-di-NACyS-DA (**7**). In view of our observation that the rate constant for the addition of NACySH to DA quinone is at least 100 times greater than that for the addition of NACySH to the adduct quinone, it is somewhat surprising that any 2,5-di-NACyS-DA is formed under our reaction conditions. If homogeneous electron transfer is rapid (Eq. [5]), then the most rational explanation requires the equilibrium constant for the oxidation of the monoaddition adduct by DA quinone (Eq. [6]) to be larger than the estimate of 1 at pH 2.0 and to increase with increasing pH.

Although the 2-cysteinyldopamine adduct has not been reported previously to our knowledge, a similar C(2) addition adduct, 2-cysteinyldopa, has been obtained from 3,4-dihydroxyphenylalanine (dopa) quinone generated enzymatically using mushroom tyrosinase (*14*). 2-Glutathionyldopa has also been obtained from the tyrosinase-catalyzed conjugation of dopa with glutathione (*15*). It also has been reported that tyrosinase-generated dopa quinone reacts with protein sulfhydryl groups (*16*), but the structure(s) of the adduct(s) formed is unknown.

Other adducts that might be formed are the C(6) monoaddition and the C(2), C(5), C(6) triaddition adducts. However, no C(6) addition adduct was detected and no such C(6) addition product has been reported for the reaction of either DA quinone with L-cysteine (*11*) or in studies of the oxidation of catechol, 4-methylcate-

chol and *N*-acetyldopamine with L-cysteine (*17*). On the other hand, 6-cysteinyldopa and 6-glutathionyldopa have been detected in the tyrosinase-catalyzed oxidations of dopa (*14*, *15*).

While the formation of a triaddition adduct is possible, our conditions do not favor its formation. CA of DA in the presence of NACySH reveals that the reaction of the first molecule of nucleophile with DA quinone to form monoaddition adducts is much faster than the addition of a second molecule of nucleophile. Accordingly, the addition of a third molecule would be expected to be even slower. Also, there is a deficiency of oxidant (unreacted DA quinone) for oxidation of the diaddition adduct to its quinone, which is an advantage of this study in terms of preventing subsequent reactions of the initial products. However, under the conditions of a continuous electrochemical oxidation, a diaddition adduct of L-cysteine and DA cyclized at the C(6) position has been detected (*11*).

In summary, this study has delineated the initial reactions of DA quinone and NACySH. Previously, the pathway for the initial reaction of DA quinone with L-cysteine had been proposed to be the addition of L-cysteine exclusively to C(5) of DA quinone (*11*). However, we have shown that other nucleophilic additions also occur, including addition to C(2) of DA quinone and formation of the C(2), C(5) diaddition adduct.

ACKNOWLEDGMENTS

The authors thank B. Plashko for performing FAB–MS experiments and M. Collinson for providing the BAS-100W electrochemical system. We are grateful to T. L. Hopkins and T. Morgan for assistance with this study and for reviewing the manuscript. We also thank G. Dryhurst (University of Oklahoma) and M. Sugumaran (University of Massachusetts Boston) for critical comments about the manuscript. This research was supported in part by National Science Foundation Grants DCB-9019400, MCB-9418129, and CHE-9216101.

REFERENCES

1. Nagatsu, T. (1986) *in* Quantitative Analysis of Catecholamines and Related Compounds (Krstulovic, A. M., Ed.), pp. 209–210, Ellis Horwood Limited, Chichester.
2. Hopkins, T. L., and Kramer, K. J. (1992) *Annu. Rev. Entomol.* **37,** 273–302.
3. Graham, D. G. (1978) *Mol. Pharmacol.* **14,** 633–643.
4. Hirsch, E., Graybiel, A. M., and Agid, Y.A. (1988) *Nature* **334,** 345–348.
5. Kastner, A., Hirsch, E. C., Lejeune, O, Javoy-Agid, F., Rascol, O., and Agid, Y. (1992) *J. Neurochem.* **59,** 1080–1089.
6. Zhang, F., and Dryhurst, G. (1993) *Bioorg. Chem.* **21,** 392–410.
7. Tse, D. C. S., McCreery, R. L., and Adams, R., N. (1976) *J. Med. Chem.* **19,** 37–40.
8. Hastings, T. G., and Zigmond, M. J. (1994) *J. Neurochem.* **63,** 1126–1132.
9. Hastings, T. G. (1995) *J. Neurochem.* **64,** 919–924.
10. Fornstedt, B., Bergh, I., Rosengren, E., and Carlsson, A. (1990) *J. Neurochem.* **54,** 578–586.
11. Zhang, F., and Dryhurst, G. (1994) *J. Med. Chem.* **37,** 1084–1098.
12. Van Swaay, M. (1978) *J. Chem. Ed.* **55,** A7–A12.
13. Hawley, M. D., and Feldberg, S. W. (1966) *J. Phys. Chem.* **70,** 3459–3464.
14. Ito, S., and Prota, G. (1977) *Experientia* **33,** 1118–1119.
15. Ito, S., Palumbo, A., and Prota, G. (1985) *Experientia* **41,** 960–961.
16. Kato, T., Ito, S., and Fujita, K. (1986) *Biochim. Biophys. Acta* **881,** 415–421.
17. Sugumaran, M., Dali, H., and Semensi, V. (1989) *Arch. Insect Biochem. Physiol.* **11,** 127–137.